SLAC-PUB-14030

Proton-Nucleus Scattering Approximations and Implications for LHC Crystal Collimation*

Robert J. Noble

Stanford Linear Accelerator Center, Stanford University
2575 Sand Hill Road, Menlo Park, California 94025 USA

Abstract

In particle accelerators, scattered protons with energies close to the incident particles may travel considerable distances with the beam before impacting on accelerator components downstream. To analyze such problems, angular deflection and energy loss of scattered particles are the main quantities to be simulated since these lead to changes in the beam's phase space distribution and particle loss. Simple approximations for nuclear scattering processes causing limited energy loss to high-energy protons traversing matter are developed which are suitable for rapid estimates and reduced-description Monte Carlo simulations. The implications for proton loss in the Large Hadron Collider due to nuclear scattering on collimation crystals are discussed.

* Work supported by Department of Energy contract DE-AC03-76SF00515.

1. Introduction

Nuclear scattering processes causing limited energy loss to high-energy protons traversing matter are of interest in many applications. In high-energy particle accelerators, scattered protons with energies close to the incident particles may travel considerable distances with the beam before randomly impacting on accelerator components downstream. This spreads radiation and may damage sensitive equipment like superconducting magnets. Angular deflection and energy loss of scattered particles are the main quantities to be simulated since these lead to changes in the beam's phase space distribution and particle loss. Although very complete Monte Carlo codes exist for calculating proton-matter interactions in detail [1-3], one often requires simple estimates of cross sections, interaction lengths, root mean square (rms) scattering angles, and average energy loss as a function of atomic weight and proton momentum. Simplified proton scattering formulas are not collected in a single well-documented reference to our knowledge even though these are regularly needed in many applications. In this paper, we develop approximations valuable for rapid estimates and reduced-description, fast Monte Carlo simulations. We illustrate use of the formulas for calculating nuclear scattering losses in proposed crystal collimators for the Large Hadron Collider (LHC).

So-called particle-matter "emulation" routines within accelerator tracking codes are used to propagate high energy particles over a length of matter in one step to rapidly simulate interactions with simple decision-tree formulas and random number generators. Emulation routines are basically reduced-description Monte Carlo algorithms in which detailed particle trajectories are replaced by macroscopic orbits and only limited information about the outgoing proton is sought. These codes are particularly popular in proton-crystal collimation and volume reflection (VR) experiments where there is a need for rapid on-line analysis of a circulating proton beam [4]. The single step approach is valid because the crystal lengths are typically much less than the nuclear interaction length.

The basic processes of interest for protons traversing solids are Coulomb scattering (primarily from nuclei), energy loss from electron collisions, nuclear elastic scattering, nuclear quasi-elastic scattering (proton excites nucleus but no particle production), single diffractive inelastic scattering (particle production but proton remains intact), and hard nuclear inelastic scattering, which typically leads to loss of the incident proton from the beam. Simple formulas for multiple Coulomb scattering and energy loss are well documented, such as in the Particle Data Booklet (henceforth denoted as the PDB, Ref. 5), and large-angle single Coulomb scattering was discussed long ago in the standard text of Jackson [6]. But simplified nuclear scattering formulas are not uniformly implemented or documented, and we develop the necessary formulas in this paper. To this end, we extract the leading order behavior of nuclear differential and total cross sections in terms of atomic weight, proton momentum, and momentum transfer from data and fits in the literature. In each case, the nuclear cross sections can be written in terms of the fundamental pp elastic and single diffractive cross sections. As an application of the formulas, particle loss in the LHC (7 TeV proton beam) from nuclear scattering in crystal collimators is discussed. The magnitude of the nuclear scattering angles and energy loss leads to the conclusion that the vast majority of nuclear scattered protons in the crystals are lost on the transverse aperture limits of the LHC ring.

The case of silicon is a useful example to illustrate the relative magnitude of the different nuclear scattering processes. Silicon (A= 28, Z = 14, ρ = 2.33 g/cc) is a common crystal for proton channeling and volume reflection experiments. From the PDB [5], one finds that the total "nuclear collision length" for a proton (or neutron) incident on Si is quoted as λ_T =70.6 g/cm^2. This is a density-independent quantity given by A(grams)/($N_A\sigma_T$ (cm^2)), where A(grams) is the atomic weight, N_A is Avogadro's number, and σ_T (cm^2) is the total nuclear cross section. The nuclear collision length takes into account scattering from all nuclear processes (p+A $\rightarrow$ anything). The collision mean free path is defined by L_T (cm) = λ_T (g/cm^2) /ρ(g/cc), where ρ is the mass density. This gives us the probability P for any nuclear interaction (be it elastic or inelastic) over a given crystal length (P = 1-exp (-z/L_T)). For silicon, one finds that L_T (cm) = 30.3 cm and σ_T = 659 mb, where 1 milli-barn =

10^{-27} cm^2. The PDB numbers are for protons in the lab energy range of about 100 GeV to a few hundred GeV where the cross sections begin to change only logarithmically with lab momentum. The other nuclear length from the PDB is the "nuclear interaction length" for Si, λ_I =106 g/cm^2, which refers to all inelastic processes (p+A → A′+X). This corresponds to an inelastic mean free path of L_I (cm) = 45.5 cm and cross section σ_I = 439 mb. Inelastic processes are the predominant nuclear effect for protons traversing a crystal. For a hypothetical 1 cm long crystal, about 2% of the incident beam is lost to inelastic scattering.

Most inelastic events lead to total loss of the incident proton from the beam, and a spray of hadronic states exiting the crystal, much of which impact beamline elements directly downstream. But a special subset of inelastic events is due to the so-called "single diffractive" scattering of the proton in which the nuclear target is excited to a low-mass state (p+A → p+A′+X), massive particles X are produced, and the incident proton survives, losing only a small amount of energy with a slight change in direction. As we show in Section 5, the single diffractive cross section for Si is about 11 mb at 200 GeV, corresponding to a remarkably small 2.5% of all inelastic events. Finally the difference between the total nuclear cross section and the inelastic cross section accounts for all so-called nuclear "elastic" (p+A → p+A) and "quasi-elastic" events (p+A → p+A* with no particle production but A* emits photons or ejects nucleons), $\sigma_T - \sigma_I = \sigma_{el} + \sigma_Q$ = 220 mb. The corresponding mean free path is L_{el+Q} (cm) = 90.8 cm for Si. For a 1 cm long crystal, about 1% of the incident beam undergoes elastic plus quasi-elastic scattering with negligible energy loss but some angle deviation. Note that 97% of the incident beam participates in no nuclear interactions whatsoever within the hypothetical 1 cm long Si crystal at these energies.

Strictly speaking the results in this paper are for protons traversing an amorphous solid in which the particle's orbit takes it randomly close to nuclei throughout the solid. For crystals a complication arises in calculating nuclear interactions when the proton is on a channeling trajectory between atomic planes or crosses planes at a small angle. Then the proton can traverse long distances without ever coming near a nucleus. The results we present in this paper based on fundamental nuclear cross sections can still be used, but one must take into account that the proton sees a lower effective density along its trajectory, and the effective mean free path L increases. Experimentally one does observe reduced nuclear scattering for these particles. Reduced scattering occurs for angles less than about $6\theta_c$ relative to a crystal plane, where θ_c is the planar critical channeling angle [7]. For larger angles, the average scattering is found to be essentially the same as for an amorphous material. In a simulation the first-order correction is to change the local mass density sampled by the particle to $\eta(\theta)\ \rho$(g/cc), where $\eta(\theta)$ is a smooth function with range $0 < \eta(\theta) \leq 1$ for angles $0 \leq \theta \leq 6\theta_c$, and $\eta(\theta) = 1$ for $\theta > 6\theta_c$.The effect of this is to make the mean free paths longer, but it will not change rms angles or rms energy loss calculated for the fundamental scattering mechanisms.

This paper is organized as follows. In Section 2, we briefly review the formulas for the nuclear total and inelastic cross sections at energies above 100 GeV. In Section 3, we describe the elastic scattering formulas and make a special separation of multiple and large angle Coulomb scattering from the nuclear scattering to simplify the rms angle calculations within a simulation. In Section 4, we cover quasi-elastic scattering, which has as its basis the fundamental pp interaction, and express the nuclear scattering formulas in terms of the pp elastic cross section. In Section 5, nuclear single diffractive scattering is discussed, and formulas for the scattering angle, diffractive mass, and proton energy loss in the lab are derived. The technique for using the simplified nuclear scattering formulas in a Monte Carlo simulation is described in Section 6, and in Section 7 we apply the scattering algorithm to the example of LHC halo beam passing through a crystal collimator. A summary of the results is given in the last section, and a sample nuclear scattering code is given in the Appendix.

2. Nuclear Total and Inelastic Cross Sections

About two-thirds of all proton nuclear events are inelastic scatterings in which particle production occurs, and the incident proton is usually lost from the beam by being transformed into other hadronic states, while still conserving charge and baryon number. For fast simulations it is important to know the probability of any nuclear reaction occurring (from σ_T) in a given thickness of material and the probability of an inelastic event occurring (from σ_I) which usually leads to loss of the proton.

The total and inelastic cross sections as functions of atomic weight A and proton laboratory momentum p are well known experimentally, and we quote the simple formulas valid for momentum above 100 GeV/c and elements from carbon and higher. These two nuclear cross sections are commonly parameterized in terms of the total proton-proton cross section. For $p \geq 100$ GeV/c, the total pp cross section is approximately [8]

$$\sigma_T{}^{pp}(\text{mb}) = 26.3 + 2.33\ ln\ p(\text{GeV/c}).$$

The total nuclear cross section is approximately $\sigma_T{}^{pA} = 1.31\ A^{0.77}\ \sigma_T{}^{pp}$, and the inelastic cross section is $\sigma_I{}^{pA} = 1.06\ A^{0.71}\ \sigma_T{}^{pp}$, using the experimentally determined A dependences. The numerical factors are chosen to give the cross sections in the PDB [5] at 200 GeV/c.

3. Nuclear Elastic Scattering

About a third of all high-energy nuclear events are elastic and quasi-elastic scatterings in which no particle production occurs, and the proton is simply deflected by the nucleus. Nuclear elastic scattering involves a "coherent" interaction of the proton with the whole nucleus while quasi-elastic scattering (also called incoherent scattering) originates from the short distance pp scattering. The differential cross section is roughly separable into two contributions from these processes according to small and large lab scattering angle θ or equivalently, square of the invariant momentum transfer $t \approx -p^2\ \theta^2$, where p is the lab momentum [9, 10]. Figure 1 summarizes (on a log-linear plot) the general behavior of the proton-nucleus cross section versus t. This figure summarizes the simplified cross section formulas developed in this paper. The demarcation between elastic and quasi-elastic behavior is at a momentum transfer $t \approx t_0$ corresponding to the nuclear radius. Quasi-elastic scattering is not distinguishable from elastic scattering at low t unless the photons or nuclear fragments from the nuclear excitation are detected. The separation of these two processes is useful for deriving simple rms angle formulas, allowing us to approximately separate the scattering physics within a simulation.

As $t \rightarrow 0$, the elastic cross section becomes dominated by Coulomb scattering, $d\sigma/dt \sim 1/(p^4\ \theta^4)$. For fast simulations we want to roughly separate Coulomb and nuclear elastic scattering to simplify the algorithms. The demarcation between the Coulomb and nuclear elastic behavior is at a momentum transfer $t \approx t_C$ corresponding to the forward ($t \rightarrow 0$) nuclear elastic and Coulomb scattering amplitudes being approximately equal, $\sigma_T{}^{pA}/2h \approx \alpha Z h/\pi t$, where Z is the atomic number, $\alpha \approx 1/137$ is the fine structure constant, and h is the Planck constant [8]. For silicon, Coulomb scattering dominates below $-t_C \approx 0.0015\ (\text{GeV/c})^2$. Formulas for Coulomb scattering are available in the literature [5, 6, 10], and we quote the relevant results here as needed for the simulations of Section 7. The important point for proton-matter simulations is that the total Coulomb cross section is several orders of magnitude greater than for nuclear processes. Coulomb collisions are so numerous that they are usually treated in the multiple scattering approximation while nuclear processes are treated as single events in a simulation. The number of Coulomb collisions is much greater than one for targets as thin as 10^{-3} radiation lengths (down to ~94 microns in Si). There is a high probability for many small-angle scatterings, and the distribution of angles due to this multiple Coulomb scattering (MCS)

is well approximated by a standard Gaussian distribution. The MCS rms angle in each plane over a thickness Δz is $<\theta'^{2}>_{MCS}^{1/2} \approx [13.6/p(GeV/c)](\Delta z/X_0)^{1/2}\ (1+0.038\ ln\ (\Delta z/X_0))$ mrad, where X_0 is the radiation length (9.36 cm for Si) [5]. The exception is occasional large-angle Coulomb scattering which adds a small tail to the Gaussian distribution for plane-projected angles $\theta' > 2.5\ \sqrt{2}\ <\theta'^{2}>_{MCS}^{1/2}$. This separation of the angular distribution into two components is fully described by Jackson [6], and his distribution function can be used to simulate large angle single scattering. The single scattering distribution is

$$P_s(\theta') = 1/(8\ ln\ (204\ Z^{-1/3}))\ (\sqrt{2}\ <\theta'^{2}>_{MCS}^{1/2}/\theta')^3.$$

The total probability for a large angle scattering (includes both signs) greater than $2.5\ \sqrt{2}\ <\theta'^{2}>_{MCS}^{1/2}$ is $P = 1/(2.5^2\ 8\ ln\ (204\ Z^{-1/3})) \approx 4.5E\text{-}3$ for most elements.

Next we consider the nuclear scattering component. For carbon and higher elements, the total nuclear elastic cross section is well approximated by multiplying the proton-proton elastic cross section by the atomic weight A of the material, $\sigma_{el}^{pA} = A\ \sigma_{el}^{pp}$. This fits the integrated cross sections of Schiz et al [11] to a few percent. The linear A dependence is what we expect for a coherent nuclear process in which all nucleons participate in the scattering. In this approximation, all momentum dependence is contained in the pp elastic cross section. The pp cross section is experimentally well determined, and for lab momentum above 100 GeV/c is approximated by the form [8]

$$\sigma_{el}^{pp}(mb) = 0.175\sigma_T^{pp}(mb) = 0.175[26.3 + 2.33\ ln\ p(GeV/c)]\ .$$

For example at 200 GeV/c, $\sigma_{el}^{pp} = 6.76$ mb and the nuclear elastic cross section for Si is about 189 mb. This only rises to 208 mb at 1 TeV. The nuclear elastic mean free path is given by $L_{el}\ (cm) = A(grams)/(N_A\ \sigma_{el}^{pA}(cm^2)\ \rho(g/cc))$, which gives us the probability P for a particle to elastically scatter over a given crystal length, $P = 1\text{-}\ exp\ (-z/L_{el})$. For silicon at 200 GeV/c, $L_{el}\ (cm) = 106$ cm.

To calculate the mean square angular deflection in θ for any particular process, we need the differential cross section $d\sigma/dt \approx (-\pi/p^2)\ d\sigma/d\Omega$ (if no φ dependence) corresponding to that type of scattering. The mean square angular deviation is $<\theta^2> = (1/\sigma) \int \theta^2\ (d\sigma/d\Omega)\ d\Omega$. For simple analytic estimates or reduced-description simulations, we only need the gross behavior of the differential cross section and not the detailed behavior, making sure that our estimate gives the correct total cross section. The general behavior of high-energy proton-nucleus cross sections are well illustrated in Figure 3 of Van Ginneken [10] for 175 GeV/c protons on different elements. The demarcation between the predominantly elastic and quasi-elastic regions in the differential cross section occurs at a momentum transfer corresponding roughly to the inverse nuclear radius, $\sqrt{-t_0} \approx \sqrt{[0.45\ /A^{2/3}\ (GeV/c)^2]} \approx h/(1.3\ R_{nuc})$, where $R_{nuc} \approx 1.4\ A^{1/3}$ fermi ($f = 10^{-13}$ cm). The cross sections drop off exponentially with t but with different slopes for elastic and quasi-elastic scattering. Physically this is because elastic scattering has a length scale characteristic of the full nuclear radius while quasi-elastic scattering (higher t) is probing the shorter range nature of nucleon-nucleon elastic scattering.

From the slope fits of Schiz et al [11], a good approximation to the elastic differential cross section for the elements from carbon and higher is

$$d\sigma_{el}^{pA}/dt \approx 12.9\ A^{5/3}\ \sigma_{el}^{pp}\ exp(12.9A^{2/3}\ t)\ \ mb/(GeV/c)^2,$$

where $t \approx -p^2\ \theta^2$ is defined with a minus sign and is in units of $(GeV/c)^2$. The pre-factors are chosen such that upon integrating over t from 0 to $-\infty$, this form yields the above-mentioned total cross section σ_{el}^{pA}. The slope factor $12.9A^{2/3} \sim R_{nuc}^{-2}$ in the exponent is just that expected for the diffractive effect of the nuclear radius: larger objects elastically scatter with smaller angles. We have omitted any dependence of the slope on center-of-mass energy squared, s, since according to the data from 70 to 175 GeV/c [10, 11] for carbon and higher, the slopes are only weakly dependent on s (at most a *ln*

s dependence). Given the approximations we have made for $d\sigma_{el}^{pA}/dt$ we can ignore this correction up to the few-TeV scale. The above expression captures the major dependency on proton lab momentum (within σ_{el}^{pp}), atomic weight A, and momentum transfer squared t for nuclear elastic scattering. Our approximation also omits the diffractive interference effects for the heavier elements (copper and higher) associated with the nuclear radius. But this contribution occurs over a very limited t-range around $t \approx t_0$ (see Fig. 3 in Ref. 10), and it has little impact on the calculation of total cross section or averages like $<\theta^2>$, which are dominated by the cross section peaking at t = 0.

The mean square lab angle for nuclear elastic scattering is calculated from the integral $<\theta^2>_{el} = (1/\sigma_{el}^{pA}) \int \theta^2 (d\sigma_{el}^{pA}/d\Omega)\, d\Omega$, and the θ integral is extended from 0 to ∞. Substituting for the differential cross section we get

$$<\theta^2>_{el} \approx (1/ A\, \sigma_{el}^{pp}) \int \theta^2 (p^2/\pi) (12.9\, A^{5/3}\, \sigma_{el}^{pp}) \exp(-12.9 A^{2/3}\, p^2\, \theta^2)\, \theta d\theta\, d\varphi \approx 1/ (12.9 A^{2/3}\, p^2)\ \text{rad}^2,$$

where p is the lab momentum in GeV/c. This is the square of the full scattering angle, and if one needs the projection on either transverse plane then this is multiplied by 1/2. As an example for silicon at 100 GeV, the elastic rms angle for each plane is $<\theta^2>_{x,y}^{1/2} = 197 / (A^{1/3}\, p(\text{GeV/c}))$ mrad ≈ 0.65 mrad.

4. Nuclear Quasi-Elastic Scattering

Since it does not involve particle production, nuclear quasi-elastic (QE) scattering typically results in a negligible energy change (~MeV) for the proton. The nucleus is excited by the proton scattering on an internal nucleon, either promoting it to a higher level in the nuclear potential where it later emits a photon, or causing nuclear fragments to be ejected out of the nucleus. Quasi-elastic scattering has as its basis the fundamental pp elastic interaction, and this can be used to parameterize the p-nucleus QE cross section.

Figure 3 of Van Ginneken [10] contains the key information to extract $d\sigma_Q^{pA}/dt$ and σ_Q^{pA}. The momentum transfer and proton deflection angle for QE scattering are larger than for the coherent elastic scattering. Below the ankle break point at $t = t_0$ in the cross section, quasi-elastic scattering becomes experimentally difficult to distinguish from elastic scattering, relying on the detection of low-energy photons or nuclear fragments emitted by the excited nuclear state. But theoretical and experimental information suggest that the QE differential cross section does remain finite as $t \rightarrow 0$ [9]. To capture the general behavior suitable for simple calculation, we parameterize the quasi-elastic cross section by an exponential in t continuing smoothly to t = 0. From the slope fits in Ref. 10, a good approximation to the differential cross section for the elements from carbon and higher is

$$d\sigma_Q^{pA}/dt \approx 10\, \sigma_Q^{pA} \exp(10\, t)\ \ \text{mb/(GeV/c)}^2,$$

where t is defined with a negative sign and is in units of $(\text{GeV/c})^2$. The slope factor $b = 10\ (\text{GeV/c})^{-2}$ is what we would expect for pp elastic scattering at the 0.1 - 1 TeV/c scale and t of order 0.05 - 0.2 $(\text{GeV/c})^2$ [8] . We have omitted any *ln* s dependence in the slope factor, which like the elastic case, is a negligible correction within our approximations even up to the few-TeV scale. From the data in Refs. 10 and 11 there appears to be no significant A dependence in the slope parameter, consistent with the scattering being due to a single pp (or p-n) scattering occurring within the nucleus.

An integration of the Van Ginneken curve fits for $d\sigma_Q^{pA}/dt$ yields the an approximate expression for the total cross section $\sigma_Q^{pA} = 0.78\, A^{1/2}\, \sigma_{el}^{pp}$, where σ_{el}^{pp} is the pp elastic cross section. The $A^{1/2}$ dependence indicates that QE scattering is more determined by interactions at the nuclear periphery and rather than over the entire disk area ($\sigma \sim A^{2/3}$). As a check we find that this formula is consistent with the sum $\sigma_{el} + \sigma_Q$ being equal to $\sigma_T - \sigma_I$ from the PDB [5] for elements from carbon and higher at the level of 5%. For example at 200 GeV/c, the total quasi-elastic cross section for Si is

calculated to be $\sigma_Q{}^{pA} \approx 28$ mb. Adding this to the elastic cross section of 189 mb found earlier, we find the sum of the elastic and quasi-elastic cross sections agree closely with the PDB average value of 220 mb quoted in the Introduction. The nuclear quasi-elastic mean free path is given by $L_Q\,(\text{cm}) = A(\text{grams})/(N_A\,\sigma_Q{}^{pA}(\text{cm}^2)\,\rho(\text{g/cc}))$. The mean free path tells us the probability for a particle to quasi-elastically scatter over a given crystal length ($P = 1- \exp(-z/L_Q)$). For silicon at 200 GeV/c, one finds that $L_Q\,(\text{cm}) = 713$ cm.

The mean square lab angle for nuclear quasi-elastic scattering is calculated from the integral $\langle\theta^2\rangle_Q = (1/\sigma_Q{}^{pA}) \int \theta^2\,(d\sigma_Q{}^{pA}/d\Omega)\,d\Omega$, and the θ integral is extended from 0 to ∞. Substituting for the differential cross section we get

$$\langle\theta^2\rangle_Q \approx (1/\sigma_Q{}^{pA}) \int \theta^2\,(p^2/\pi)\,10\,\sigma_Q{}^{pA} \exp(-10\,p^2\,\theta^2)\,\theta d\theta\,d\varphi \approx 1/(10\,p^2)\ \text{rad}^2\ ,$$

where p is in GeV/c. The QE scattering angle is independent of A within our approximations. This is the square of the full scattering angle, and if one needs the projection on either transverse plane then this is multiplied by 1/2. At 100 GeV the quasi-elastic rms angle for each plane is $\langle\theta^2\rangle_{x,y}{}^{1/2} = 224/p(\text{GeV/c})$ mrad ≈ 2.2 mrad.

5. Nuclear Single Diffractive Inelastic Scattering

Most inelastic scattering results in a large energy transfer to the nucleus, particle production, and a loss of the incident proton. Single diffractive (SD) inelastic scattering involves particle production, but the incident proton retains its identity despite losing some energy (p+A → p+A′+X, and X= massive particles). It is a rare subset of all inelastic events, typically accounting for a few percent of the total inelastic cross section. This scattering is fundamentally a single pp (or pn) interaction within the nucleus. The SD pp cross section can be used to parameterize the p-nucleus cross section, just as the elastic pp cross section was used to describe QE scattering.

From Figure 4 in Ref. 10, we extract the approximation for the nuclear SD cross section, $\sigma_{SD}{}^{pA} = A^{1/2}\,\sigma_{SD}{}^{pp}$, where

$$\sigma_{SD}{}^{pp}(\text{mb}) = 0.6\,(1+36/s)\,[0.5/(1+ m_p{}^2) + \mathit{ln}\,(0.1\ s/(1+ m_p{}^2))]$$

is the pp single diffractive cross section (p+p → p+X, and X = massive particles), $s = 2\,m_p(m_p+E_p)$ is the center-of-mass (CM) energy in GeV^2, and m_p is the proton mass in GeV. We have corrected an apparent typographical error in Eqn. 12 of Ref. 10. The $A^{1/2}$ dependence of σ_{SD} is a good fit for proton lab momentum up to about 10 TeV/c. This A dependence indicates that SD scattering, like the QE case, is more determined by interactions at the nuclear periphery. At 200 GeV/c, $\sigma_{SD}{}^{pp} \approx 2.1$ mb, and for silicon we obtain $\sigma_{SD}{}^{pA} \approx 11$ mb. The nuclear SD mean free path is $L_{SD}\,(\text{cm}) = A(\text{grams})/(N_A\,\sigma_{SD}{}^{pA}(\text{cm}^2)\,\rho(\text{g/cc}))$. This tells us the probability for a particle to undergo a single-diffractive scattering over a given crystal length ($P = 1- \exp(-z/L_{SD})$). For silicon at 200 GeV/c, one finds that $L_{SD}\,(\text{cm}) = 1814$ cm.

The complete SD differential cross section has both a t-dependence and a dependence on the mass of the diffractively produced state. This makes the approximations needed for a fast Monte Carlo code more complicated. We use the diffractive pp scattering as a guide to the p-nucleus scattering cross section dependencies. Experimentally the SD differential cross section for pp varies like exp(bt), with the slope b weakly dependent on s (~ log s), and it remains finite all the way down to t = 0. There is some dependence of b on the mass M of the diffractively produced state, but for $M^2 > 1+ m_p{}^2$, which accounts for the vast majority of SD events, the slope factor is approximately 7 $(\text{GeV/c})^{-2}$ [8, 10]. We parameterize the SD cross section for p-nucleus scattering versus t by a single exponential for all M and continue it to t = 0,

$$d\sigma_{SD}^{pA}/dt \approx 7\,\sigma_{SD}^{pA} \exp(7t) \ \text{mb/(GeV/c)}^2,$$

where t is defined with a negative sign and is in units of $(GeV/c)^2$. All elements are found to have the same SD slope factor consistent with the scattering being due to single pp (or p-n) scattering [10].

The mean square lab angle for nuclear single diffractive scattering is calculated from the integral $\langle\theta^2\rangle_{SD} = (1/\sigma_{SD}^{pA}) \int \theta^2 \, (d\sigma_{SD}^{pA}/d\Omega) \, d\Omega$, and the θ integral is extended from 0 to ∞. Substituting for the differential cross section we get $\langle\theta^2\rangle_{SD} \approx 1/ (7\ p^2)$ rad^2, where p is in GeV/c. This is the square of the full scattering angle, and if one needs the projection on either transverse plane then this is multiplied by 1/2. At 100 GeV the single diffractive rms angle for each plane is $\langle\theta^2\rangle_{x,y}^{1/2}$ = 267/p(GeV/c) mrad ≈ 2.7 mrad.

The more interesting aspect of SD scattering is the energy loss experienced by the incident proton as the result of particle production. We use the double differential cross section in Ref. 10 for SD pp scattering $d^2\sigma_{SD}^{pp}/dM^2\,dt$ integrated over t to calculate the invariant mass M of the produced massive particle state. Then we make an approximate transformation to the lab frame assuming small angle scattering to obtain the final proton energy. Implicit in this simplified approach is that we omit any correlation between energy loss and scattering angle (a next order correction when needed for more detailed codes).

We do not reproduce Eqn. (10) from Ref. 10 for the pp double differential cross section here, which the reader can refer if necessary. Integrating the said expression in t, we obtain the differential cross section with respect to the invariant mass squared of the produced state as

$$d\sigma_{SD}^{pp}/dM^2 = 0.6\,(1+36/s)\,(M^2 - m_p^2)\,/\,(1+ m_p^2) \ \text{mb/(GeV)}^2 \text{ , for } M^2 \le 1+ m_p^2$$

and

$$d\sigma_{SD}^{pp}/dM^2 = 0.6\,(1+36/s)\,/\,M^2 \ \text{mb/(GeV)}^2 \text{ , for } M^2 \ge 1+ m_p^2.$$

Here $s = 2\ m_p(m_p+E_p)$ is the CM energy squared in GeV^2, and all masses are in GeV. Note the differential cross section is 0 for $M^2 \le m_p^2$, which is the kinematic limit since the final produced state must have at least the mass of the original proton. Integrating $d\sigma_{SD}^{pp}/dM^2$ from m_p^2 up to a limit M^2 = s/10 gives the earlier quoted expression for σ_{SD}^{pp}. The upper limit comes from the requirement that the incident proton remains intact. For $M^2 >$ s/10 the probability becomes high that the proton changes state, and this is no longer a single-diffractive scattering event [8, 10]. Although the mass distribution is not Gaussian, the mean square invariant mass of the SD-produced state (in GeV^2) is useful for estimating the energy loss of scattered protons,

$$\langle M^2\rangle_{SD} = (1/\sigma_{SD}^{pp}) \int M^2 \, (d\sigma_{SD}^{pp}/dM^2)\, dM^2$$

$$= 0.6\,(1+36/s)\,(1/\sigma_{SD}^{pp})\,[0.1s - (1+ m_p^2) + (1/3+ m_p^2/2)\,/\,(1+ m_p^2)]$$

$$= [0.1s - (1+ m_p^2) + (1/3+ m_p^2/2)\,/\,(1+ m_p^2)]\,/\,[0.5/(1+ m_p^2) + \mathit{ln}\,(0.1\ s/(1+ m_p^2))].$$

For example at 200 GeV, we find that $\langle M^2\rangle_{SD}$ = 11 GeV^2. At energies above 3 TeV, the expression can be replaced by its asymptotic limit $\langle M^2\rangle_{SD} \approx 0.1s\ /\ \mathit{ln}\ (0.1\ s/(1+ m_p^2))$, expressed in GeV^2, accurate to better than 5%. The dependence on the integration cutoff (0.1s) is a direct result of kinematically separating out single-diffractive particle production from all other hadronic processes that naturally overlap partially in phase space.

For a given invariant mass of the SD state, we can calculate the final energy of the scattered proton in the lab frame. This is standard two-body kinematics with a transformation from the CM to lab frame for p+p → p+X. Normally we would have to consider the general case of arbitrary scattering angles, but assuming high energies and small scattering angles for the proton, the analysis is simplified in the limit of forward scattering. We need only apply conservation of energy and longitudinal momentum in the lab frame, neglecting the small transverse momentum,

$$E_0 \equiv E_i + m_p = E_f + E_x \qquad \text{and} \qquad p_i = p_f + p_x \,,$$

where the subscript i refers to the incident proton, subscript f refers to the outgoing proton, and subscript x refers to the SD-produced state. We want to solve for the final proton energy E_f in terms of E_i , p_i , m_x , m_p, so we rewrite

$$(E_i + m_p - E_f)^2 = E_x^2 = p_x^2 + m_x^2 = (p_i - p_f)^2 + m_x^2 = (p_i - \sqrt{(E_f^2 - m_p^2)})^2 + m_x^2 \,.$$

From this we get the quadratic equation: $4\ s\ E_f^{\,2} - 4\ E_0\ \Sigma\ E_f + \Sigma^2 + 4\ p_i^2\ m_p^2 = 0$, where $\Sigma = s + m_p^2 - m_x^2$ and $s = 2\ m_p(m_p+E_i)$. The solution for the proton's final lab energy is

$$E_f = (E_0\ \Sigma + [E_0^2\Sigma^2 - s\ (\Sigma^2 + 4\ p_i^2\ m_p^2)]^{\,1/2}) \,/\, 2s \,.$$

The second root of the quadratic equation for E_f (the negative sign before square root) is omitted for our application since it corresponds to the proton having a very small kinetic energy in the lab frame. This is the case of 180-degree (backward) scattering in the CM which within our approximation for $d\sigma_{SD}^{\,pA}/dt$ implies an exponentially small scattering probability at such large angles.

The above expression for E_f is relatively simple for fast calculations, but for high energies where $s >> m_x^2$, m_p^2 we expand in powers of m^2/s to obtain the very simple formula

$$E_f \approx E_i - m_x^2/(2m_p) + m_p/2.$$

For high energy SD scattering, the proton's energy loss in the lab frame is $\Delta E \approx m_x^2/(2m_p) - m_p/2$. As an example, for E_i = 200 GeV, we find $\langle M^2\rangle_{SD}$ = 11 GeV^2 from our earlier mean square mass calculation. For $m_x^2 = \langle M^2\rangle_{SD}$, the expectation value for the proton energy loss in the lab is ΔE = 6 GeV or about 3% of its initial energy. At 7 TeV, the SD mass squared increases to $\langle M^2\rangle_{SD}$ = 192 GeV^2, and the proton energy loss is 103 GeV or 1.5%. This is an important result for high energy channeling, volume reflection, and crystal collimation. It tells us that if the transverse and longitudinal acceptances of the proton collider cannot handle a few percent of energy spread, then a large fraction of SD scattered protons will be lost from the machine. Asymptotically at high energies (> 3TeV) the relative energy loss can be written as $\Delta E/E_p \approx \langle M^2\rangle_{SD}/(2m_pE_p) \approx 0.1 \,/\, ln\ (0.2\ m_pE_p/(1+ m_p^2))$, which falls off very slowly with proton lab energy.

The fact that the produced state must have an invariant mass $m_x = M \geq m_p$ means that care must be taken to randomly assign the SD mass in a Monte Carlo simulation. The simulated mass taken as a random number does not include values down to zero. We use the standard "inverse method" [12, 13] of choosing a random mass M by inverting the cumulative probability integral of the differential cross section. This inversion is simple since the integral is an algebraic expression, piecewise continuous about the point $M^2 = 1+ m_p^2$ where the cross section $d\sigma_{SD}^{\,pp}/dM^2$ changes shape. For the low-mass range, the probability integral is integrated from m_p^2 to $M^2 \leq 1+ m_p^2$,

$$P_1 = (1/\sigma_{SD}^{pp}) \int [0.6\ (1+36/s)\ (M^2 - m_p^2) \,/\, (1+ m_p^2)]\ dM^2$$

$$= [(0.5\ M^4 - m_p^2\ M^2 + 0.5\ m_p^4) \,/\, (1+ m_p^2)] \,/\, [0.5/(1+ m_p^2) + ln\ (0.1\ s/(1+ m_p^2))].$$

This is a quadratic equation for M^2 with solution

$$M^2 = m_p^2 + \{2(1+ m_p^2)\ [0.5/(1+ m_p^2) + ln\ (0.1\ s/(1+ m_p^2))]\ P_1\}^{1/2} \,, \quad \text{for } M^2 \leq 1+ m_p^2.$$

The other root with minus sign is not physical since the mass is less than m_p. Substituting a sample of uniformly distributed random numbers P_1 in the range $[0, P_{1max}]$ will simulate the low-mass spectrum $m_p^2 \leq M^2 \leq 1+ m_p^2$. The demarcation $P_{1max} = [0.5/(1+ m_p^2)] / [0.5/(1+ m_p^2) + ln\ (0.1\ s/(1+ m_p^2))]$ corresponds to the point $M^2 = 1+ m_p^2$ where the cross section changes shape. Probabilities P_2 in the upper range $[P_{1max}, 1]$ correspond to the high-mass range obtained from the cumulative probability integral up to $M^2 \leq s/10$,

$$P_2 = P_{1max} + (1/\sigma_{SD}^{pp}) \int [0.6\ (1+36/s) / M^2\ ]\ dM^2$$

$$= [0.5/(1+ m_p^2) + ln\ (M^2\ /(1+ m_p^2))]\ \ / [0.5/(1+ m_p^2) + ln\ (0.1\ s/(1+ m_p^2))].$$

Inverting this yields the mass formula

$$M^2 = (1+ m_p^2)\ \exp\{[0.5/(1+ m_p^2) + ln\ (0.1\ s/(1+ m_p^2))]\ P_2] - 0.5/(1+ m_p^2)\}\ ,\ \text{for } M^2 \geq 1+ m_p^2.$$

Substituting a sample of uniformly distributed random numbers P_2 in the range $[P_{1max}, 1]$ will simulate the high-mass spectrum $1+m_p^2 \leq M^2 \leq s/10$.

6. Use of Formulas in Simulations

The basic procedure for using these nuclear scattering formulas in a reduced-description Monte Carlo simulation is described here. The procedure is particularly simple and robust because in a fast emulator code we are only asking for limited information regarding the proton's deflection and energy loss, without regard for details about hadronic final states. As an illustration, we have incorporated our algorithm within Yazynin's proton transport subroutine MOVE_AM of his crystal code CRY_AP.FOR [14]. A sample nuclear scattering algorithm in FORTRAN is supplied in the Appendix. Our algorithm is intended only as a pedagogical example (in silicon) and can be tailored to any proton transport code as desired. We will apply this algorithm in Section 7 to the case of protons undergoing crystal volume reflection in the LHC.

In a typical particle simulation, protons are pushed individually through a length of matter, Δz. Independent of any nuclear interactions calculated in the simulation, Coulomb scattering and energy loss are performed for every proton over this length. The MCS angle and dE/dx formulas are taken from the PDB [5]. To assign any large-angle scattering $\theta' > 2.5\ \sqrt{2}\ <\theta'^{\,2}>_{MCS}^{1/2}$ in each plane, we use Jackson's distribution formula $P_s(\theta')$ quoted in Section 3. Using a uniform random number generator we first decide if a large-angle scattering occurs in each plane ($P_{rand} \leq$ 4.5E-3). If so, then the projected angle (with random sign) is assigned by applying the inverse method [12, 13] to said distribution, $\theta' = 2.5\ \sqrt{2}\ <\theta'^{\,2}>_{MCS}^{1/2} /(1\text{-}P)^{1/2}$, where P is a uniform random number excluding 1.

For each proton entering the solid, we next calculate the probability of any nuclear interaction $P_T = \Delta z/L_T$, and using a uniform random number generator we decide if a scattering occurs ($P_{rand1} \leq P_T$). Normally no nuclear scattering occurs since P_T is a small number, and the particle traverses the material with no nuclear interaction. This method saves considerable simulation time as no further nuclear calculations are performed for most particles after this test. Practically speaking, one should keep Δz short enough that P_T is not greater than ~ 0.1 (and incidentally, short enough that Coulomb dE/dx energy loss is not too large). If the scattering probability is too high, then one should divide the crystal into more than one step to insure that only one scattering is likely to occur in Δz.

If a nuclear scattering occurs by the above random test, we then decide what type of process it is, either inelastic or not. This branch point in the decision-tree is again done with a uniform random number, and the event is inelastic if $P_{rand2} \leq P_I / P_T = \sigma_I / \sigma_T$. If not, it is an elastic or quasi-elastic event. For this case, we must choose between elastic and the rarer quasi-elastic scattering. The QE choice is made if $P_{rand3} \leq P_Q /(P_{el}+ P_Q) = \sigma_Q/(\sigma_{el} + \sigma_Q)$, and we assign the angular kick $<\theta^2>_Q^{1/2}$ to

the outgoing proton, multiplied by a Gaussian-distributed random number and a sign. If the event is elastic, then we instead assign the angular kick $<\theta^2>_{el}^{1/2}$. For the inelastic case, we have two choices: either the event is a rare single-diffractive (SD) event in which the proton losses some energy, survives, and is scattered in angle, or it is the more probable, hard inelastic event in which the proton is totally lost from the beam. The SD scattering is a subset of all inelastic events (typically 2-3% of all inelastic events), and this choice is made if $P_{rand4} \leq P_{SD}/P_I = \sigma_{SD}/\sigma_I$. In this case, the proton SD scattering angle is randomly assigned using $<\theta^2>_{SD}^{1/2}$, and its final energy E_f is calculated from the formulas in Section 5 using the randomly assigned mass $m_x = M$ of the diffractive state. If it is not an SD event, then the proton is terminated at this point in the algorithm.

7. Implications for Crystal Collimation in the Large Hadron Collider

A high-energy proton collider can stably transport particles within a limited range of transverse and longitudinal emittances, called the machine acceptance. The acceptance is limited transversely by magnetic focusing strength and vacuum pipe aperture and longitudinally by the radio-frequency (RF) bucket height that can confine a maximum energy spread. During colliding beam operations, protons normally suffer various perturbations that cause them to migrate transversely from the beam core to the halo (>5-6 σ). These protons continue to move farther off axis until they impact sensitive items like superconducting magnets or are scattered by beam-line components. This results in spreading radiation throughout the beam tunnel and heating superconducting magnets.

To limit the uncontrolled loss of halo protons in the arcs, bent-crystal volume reflection (VR) has been proposed for use in the Large Hadron Collider (7 TeV design beam energy) to continuously sweep halo particles ($r_{halo} > 5\sigma_{core}$, $\sigma_{core} \approx 0.2$ mm) in a controlled fashion into dedicated absorber-collimators. Halo protons enter a bent silicon crystal, travel to a depth where their angle relative to a to a crystal plane is nearly the critical channeling angle (θ_c), reflect off that plane, and exit along a direction opposite to the crystal's curvature and with a deflection of order θ_c ($\approx$ 2.5 micro-radian at 7 TeV in Si). Figure 2 illustrates the volume reflection effect experienced by protons in a bent crystal in terms of the standard "triangle-plot" used in crystal experiments, generated with the code CRY_AP of Yazynin [14]. The basic VR mechanism has been verified in experiments at the Tevatron and CERN SPS [4]. Crystal length and curvature are chosen to give a sufficiently large angular acceptance for halo particles. The maximum particle angle (VR acceptance) that will result in volume reflection is given by the crystal thickness divided by crystal radius. For an LHC beta function of $\beta_f \approx$ 75 m, halo particles have angles $r_{halo} / \beta_f \approx 13$ micro-rad or higher. In the LHC example below we use a 5 mm Si crystal with radius 100 m, which gives a very generous 50 micro-rad acceptance. Halo beam typically has normalized emittance $\varepsilon_N = \gamma\varepsilon \geq 100$ micron-rad. For comparison, the normalized rms emittance of the LHC beam is about 3.8 micron-rad, the core beam divergence is about 2.6 micro-rad, and the multiple Coulomb scattering angle in 5 mm of Si is about 0.4 micro-rad per plane. Coulomb energy loss is completely negligible, being only 3 MeV over the 5 mm crystal. As long as most halo protons do not suffer a large-angle nuclear scattering, the VR technique offers promise to control beam halo. But any nuclear scattered protons are a new and potentially damaging background from this collimation method, and we need good scattering estimates for these.

For those halo protons that do experience a nuclear interaction in the crystal, we can make predictions about their fate within the machine acceptance using the formulas we have developed. Losses increase linearly with crystal thickness. For our 5 mm Si crystal about 98% of the incident halo protons will suffer no nuclear scattering and will have a good chance of undergoing the intended volume reflection. About 2% of incident halo protons will experience some nuclear interaction (somewhat less for particles moving roughly parallel to the crystal planes) in the 5 mm crystal, with 2/3 of these basically stopped by an inelastic nuclear event and 1/3 having an elastic or quasi-elastic scattering but surviving. Within the inelastic events are the rare single-diffractive events in which the proton survives, being about 5E-4 of the halo particles incident on the 5 mm crystal at this energy.

For 7 TeV protons, the single-diffractive rms scattering angle is about 38 micro-rad, and the expected relative energy loss is 1.5E-2. But there is a long tail to the SD mass distribution. The largest SD energy loss for a 7 TeV proton is about 10%, corresponding to the upper bound of $M^2 = s/10$ put on our approximate SD spectrum. The LHC RF half-bucket height is $\Delta E_{RF}/E$ = 3.6E-3, and the nominal beam energy spread is $\delta E/E$ = 1E-4. A fraction of SD scattered protons lose so little energy that they actually remain within these limits. From the probability formulas in Section 6, the fraction of SD protons within the nominal beam spread is about 3%, and the fraction within the rf bucket is about 50%. The other half of SD protons may reach the rf cavities but be outside the stable longitudinal bucket. These lower energy SD protons will most likely be lost transversely because their orbit amplitude $\sigma = [(\beta_f \varepsilon + (\eta \Delta p/p)^2]^{1/2}$ has a large contribution from the dispersive term ($\eta \approx 1.5$ m). For example the SD beam fraction with $\Delta p/p$ = 3.6E-3 has $\beta_f \varepsilon \approx$ 1E-5 m^2 and $\eta \Delta p/p \approx$ 5.4E-3 m, so these protons will have $\sigma \approx 6$ mm, which is already $30\sigma_{core}$. The more representative SD population with the expected energy loss of $\Delta p/p$ = 1.5E-2 has a beam size $\sigma \approx 23$ mm. Since the LHC vacuum screen width is only 37 mm, this lower energy group will be lost with near certainty.

The elastic and quasi-elastic protons do not have a problem with dispersion, but their transverse amplitudes still grow due to scattering angle. Elastic protons are the more problematic since they are more plentiful than SD protons and QE protons, being about 0.6% of the halo beam incident on the 5 mm crystal. The un-normalized emittance of halo beam is at least $\varepsilon = (5\sigma_{core})^2/\beta_{avg} \approx$ 1.3E-8 m. The changes in the divergence and un-normalized emittance for the elastic and QE halo protons are large: $\Delta\theta_{el}$ = 9 micro-rad, $\Delta\varepsilon_{el} = \beta_f \ (\Delta\theta_{el})^2$ = 6.1E-9 m and $\Delta\theta_Q$ = 32 micro-rad, $\Delta\varepsilon_Q$ = 7.7E-8 m, respectively. So the nuclear scattering will immediately move most of these protons farther out into the halo and cause them to be randomly lost downstream even faster.

We have used Yazynin's crystal emulation code CRY_AP [14] with our new nuclear formulas added to his subroutine MOVE_AM to simulate 7 TeV protons traversing a bent crystal (sample code in the Appendix). This lets us visualize in angle-space and in phase space the effect of the crystal on the halo particles. A hypothetical halo beam slice is arbitrarily located 0.01 mm horizontally off axis with a range of angles xp0 from -0.01 mrad to +0.06 mrad. Halo protons traverse a 5 mm thick, bent Si crystal with curvature radius of 100 m. When all nuclear processes are turned OFF in the simulation, the resulting triangle plot of scattered protons is shown in Figure 3. This plot basically shows where better than 98% of the incident halo protons end up in angle space since nuclear scattering affects so few protons. The VR particles in the acceptance range xp0 = [0.0, 0.05] mrad are apparent by their deflection to the left. The main VR group is centered in the range xpout-xp0 = [-0.001, -0.005] mrad, with an average VR deflection of 3 micro-rad $\approx 1.2\theta_c$. The two "amorphous" populations with input angles outside the VR acceptance are evident in the upper and lower groupings with no net deflection. The angular spreads of the distributions are due to Coulomb scattering and additionally for the VR region, by the variation of a proton's reflection point off the channeling potential. The effect of occasional large-angle Coulomb scattering is evident from the few outliers in the angular tails, though most of these are within 10 micro-rad of the VR group. The output phase space of the halo beam slice is shown in Figure 4. The vertical line at x = 0.01 mm represents the input phase space of the initial beam slice. The horizontal band at xp = 0.05 mrad are the volume-captured and channeled protons. The narrow diagonal band proton from xp =0 to 0.05 mrad are dechanneled protons. The slightly offset VR group is diagonally located at angles xp between 0 and 0.05 mrad. This shows the difficulty of cleanly separating VR particles in phase space since the VR angle is only a few micro-radians at TeV energies, which is the typical divergence of circulating beam in a collider. One option is to use multiple crystals to build up the cumulative deflection.

The previous figures show the ideal case of VR when there is no nuclear scattering. Turning ON all nuclear scattering in addition to the Coulomb effects results in the simulated triangle plot shown in Figure 5 and the phase space plot in Figure 6. The wide scatter is due to the 0.6% of the protons that are nuclear scattered and survive passage through the crystal. In Figure 7 we plot the phase space of only these surviving nuclear scattered protons. A few protons are now scattered out to

almost 100 micro-radians from the incident halo slice, several times higher than due to large-angle Coulomb scattering. An analysis of the particles scattered in the VR acceptance region (xp0 = [0.0, 0.05] mrad) indicates that about 14% of nuclear scattered protons have small enough output angles to remain within the VR group (xpout-xp0 = [-0.001, -0.005] mrad), so they can still be collimated. About 15% of the elastics and 9% of the QE and SD protons are scattered into the VR group. The remaining 86% of protons are scattered to large angles outside the VR group so they are problematic for collimation. Furthermore the single-diffractive protons have significant energy loss (up to a maximum of about 10%) making their transport unstable in the LHC arcs. It should be noted that we introduced within the main CRY_AP code an algorithm to reduce nuclear scattering for protons travelling at small angles to the planes, mentioned in Section 1. Basically when protons are within + - 3 θ_c of a plane we omit any nuclear scattering. One could do a more careful approximation for reducing the nuclear effects smoothly as a function of angle, but for a fast simulation we want to avoid detailed trajectory calculations. For the 100 m curvature crystal, this means that there are almost no nuclear interactions for VR protons over about 1.5 mm of the 5 mm crystal. Compared to amorphous transport, we find that the nuclear interaction rate is reduced by about 30% for VR particles in this crystal.

8. Summary

We have developed simple approximations for nuclear elastic, quasi-elastic, and single-diffractive scattering suitable for rapid quantitative estimates and reduced-description Monte Carlo codes to simulate proton-matter interactions. For thin silicon targets used in many crystal experiments, the actual probability for any nuclear scattering in the amorphous solid is about $\Delta z/L_T \approx$ 1 cm/30 cm, so in these situations one is dealing with order one-percent nuclear probabilities for incident protons. At the 1 TeV scale, the relative probabilities for the different nuclear processes, where the probability for any nuclear scattering is normalized to unity, are given by the ratios: Any Scattering (=1): Inelastic (0.66): Elastic (0.30): Quasi-elastic (0.04): Single-Diffractive (0.02). The rms deflection angles for each transverse plane as a function of proton momentum are: Nuclear Elastic $\langle\theta^2\rangle_{x,y}^{1/2} = 197/(A^{1/3}\ p(\mathrm{GeV/c}))$ mrad, Quasi-elastic $\langle\theta^2\rangle_{x,y}^{1/2} = 224/p(\mathrm{GeV/c})$ mrad, and Single Diffractive $\langle\theta^2\rangle_{x,y}^{1/2} = 267/p(\mathrm{GeV/c})$ mrad. Finally the expected proton energy loss due to single-diffractive particle production at high energies is $\Delta E/E_p \approx \langle M^2\rangle_{SD}/(2m_pE_p) \approx 0.1 / \ln (0.2\ m_pE_p/(1+ m_p^2))$, which falls off very slowly with proton lab energy. At TeV scale energies, this means the expected SD energy loss is about 1-2%, but a maximum energy loss up to 10% is possible due to the tail of the SD mass spectrum. Nuclear scattering angles and energy losses are sufficiently high that we conclude that the majority of nuclear scattered protons from a crystal collimator will impact the edges of the LHC transverse acceptance. Single-diffractive protons are lost fastest due to their large energy loss but elastically scattered protons are more of a problem, being about ten times more abundant.

ACKNOWLEDGMENTS

This work was supported by the U.S. Department of Energy under contract DE-AC03-76SF00515. The author thanks Thomas Markiewicz, Johnny Ng, Walter Scandale, and James Spencer for discussions and suggestions during the course of this work. The author especially thanks Igor Yazynin (IHEP, Protvino) for generously providing an early version of his crystal simulation code CRY_AP.FOR to test our nuclear scattering algorithms and for answering questions regarding the use of his code.

APPENDIX: SAMPLE NUCLEAR SCATTERING ALGORITHM

A sample nuclear scattering algorithm in FORTRAN is supplied here using the formulas developed in this paper. As an illustration, we have incorporated our nuclear algorithm within I. Yazynin's proton transport subroutine MOVE_AM of his code CRY_AP.FOR (used with his permission) [14]. Our algorithm is intended only as a pedagogical example (in silicon) and can be tailored to any proton transport code as desired.

```
      SUBROUTINE MOVE_AM_(IS,DZ,RP,ZP,PC,WS)
C     Interaction p with amorphous target (by approximation)
C-------------------------------------------------------------
C      IS -   substance of target
C      DZ -   length of target (m)
C      R,RP,Z,ZP - coordinates at input of crystal
C      PC -   momentum of particle*c [GeV]
C      WS -   weight of particle
C      Author of code before modifications, Version A1, 2008:   I.Yazynin
C      Large Angle Coulomb scattering added: 4/15/2010, R.J.Noble, SLAC
C      New nuclear formulas added: 5/7/2010, R.J.Noble
C-------------------------------------------------------------

C. DES - dE/dx stopping energy
C. DLRI - radiation length

      COMMON/CRYS/ DLRI(4),DLYI(4),AI(4),DES(4),DLAI(4)
      COMMON/Nam_Z/  Nam,ZN
      REAL MSQSD

c  If this particle has already lost all momentum, then exit:
      IF(.NOT.(PC .GT. 0.)) GO TO 1000

c  Coulomb interaction turned ON?
         IF(ZN .GT. 0.) THEN

c  Energy lost from ionization process [GeV]
      PC = PC - DES(IS)*DZ
C. Multiple Coulomb scattering
C. DYA - rms of coulomb scattering
c     Include log length correction (R.J.Noble, 10/9/08)

      CORRMS = 0.
      IF(.NOT.(DZ.LT.3.8E-12*DLRI(IS))) CORRMS=1.+0.038*LOG(DZ/DLRI(IS))
c   MCS plane angle in mrad for this thickness:
      DYA = (13.6/PC)*SQRT(DZ/DLRI(IS))*CORRMS
      CALL RANNOR(O1,O2)
c   Assign MCS angle:
      RP = RP+DYA*O1
      ZP = ZP+DYA*O2

C.  Large Angle Coulomb Scattering (R.J.Noble, 4/15/2010)
c   Check for large angle Coulomb scattering in each plane separately:
```

```
      IF(.NOT.(RNDM(-1.).LE. 4.5E-3)) GO TO 5
     PROB1 = RNDM(-1.)
      IF(PROB1 .EQ. 1.) PROB1 = 0.
      ALPH1 = 2.5/SQRT(1.-PROB1)

c   Calculate RP angle change (mrad) with random sign:
      RP = RP+SQRT(2.)*DYA*SIGN(ALPH1,2.*RNDM(-1.)-1.)

    5 CONTINUE
      IF(.NOT.(RNDM(-1.).LE. 4.5E-3)) GO TO 10
      PROB2 = RNDM(-1.)
      IF(PROB2 .EQ. 1.) PROB2 = 0.
      ALPH2 = 2.5/SQRT(1.-PROB2)

c   Calculate ZP angle change (mrad) with random sign:
       ZP = ZP+SQRT(2.)*DYA*SIGN(ALPH2,2.*RNDM(-1.)-1.)

   10 CONTINUE
        ENDIF

c   Nuclear interactions turned ON?
      IF(NAM .EQ. 0) RETURN

C.  Nuclear interactions algorithm for Si example (R.J.Noble, 5/7/2010).

c   Total pp cross section (mb = 1E-27 cm**2)
      SIGTPP = 26.3 + 2.33*LOG(PC)

c   Silicon test case: density = 2.33 g/cc, atomic weight = 28.
       RHO = 2.33
       ATWT = 28
c   Total p-nucleus cross section (mb)
       SIGTOT = 1.31*(ATWT**0.77)*SIGTPP
c   Mean free path in meters
       DLTOT = (ATWT/(6.022E-4*SIGTOT*RHO))*0.01

c   Any nuclear scattering?
       IF(.NOT.(RNDM(-1.) .LE. DZ/DLTOT)) GO TO 1000

c   If nuclear scattering, is it inelastic event?
c   Inelastic p-nucleus cross section (mb)
       SIGI = 1.06*(ATWT**0.71)*SIGTPP
       IF(.NOT.(RNDM(-1.) .LE. SIGI/SIGTOT)) GO TO 200

c   If inelastic, is it a single diffractive event?
c   CM energy squared of the incident proton (GeV**2):
      EI = SQRT(0.88+PC**2.)
      S = 1.876*(0.938+EI)
c   Single-diffractive pp cross section (mb)
     SIGSDPP = 0.6*(1.+36./S)*(0.266+LOG(0.05319*S))
```

```
c   Single-diffractive p-nucleus cross section (mb)
      SIGSD = SIGSDPP*SQRT(ATWT)
      IF(.NOT.(RNDM(-1.) .LE. SIGSD/SIGI)) GO TO 100

c   Calculate SD angle (mrad) and energy loss (GeV) for proton:
      CALL RANNOR(O1,O2)          ! Gaussian random numbers O1,O2
      RP = RP+ 267.*O1/PC         ! SD angle in R plane[mr]
      ZP = ZP+ 267.*O2/PC         ! SD angle in Z plane[mr]
c   Assign an arbitrary weight to distinguish SD proton in main program:
       WS = 0.001

c   Calculate mass squared (GeV**2) of the single-diffractive state:
       DENOM = 0.266+LOG(0.05319*S)
       Y = RNDM(-1.)
       IF(Y .GT. 0.266/DENOM) GO TO 20
       MSQSD = 0.88+SQRT(3.76*DENOM*Y)
        GO TO 40
  20 CONTINUE
        MSQSD = 1.88*EXP(DENOM*Y - 0.266)
  40 CONTINUE

c   Calculate final proton energy (GeV) and momentum*c (GeV):
       EF = EI - (MSQSD/1.876) + 0.469
        PC = SQRT(EF**2. - 0.88)
       GO TO 110

 100 CONTINUE
c   If not SD event, Stop proton with hard inelastic event:
       WS = 0.00001
        PC = 0.
 110  CONTINUE
       GO TO 1000

 200 CONTINUE
c   Elastic or Quasi-elastic event?
c   Elastic pp cross section (mb)
       SIGELPP = 0.175*SIGTPP
c   Elastic p-nucleus cross section (mb)
       SIGEL = ATWT*SIGELPP
c   Quasi-elastic p-nucleus cross section (mb)
       SIGQ = 0.78*SIGELPP*SQRT(ATWT)
       IF(.NOT.(RNDM(-1.) .LE. SIGQ/(SIGEL+SIGQ))) GO TO 300

c   Quasi-elastic event:
c   Calculate QE angle (mrad) for proton:
      CALL RANNOR(O1,O2)          ! Gaussian random numbers O1,O2
      RP = RP+ 224.*O1/PC         ! QE angle in R plane[mr]
      ZP = ZP+ 224.*O2/PC         ! QE angle in Z plane[mr]
c   Assign an arbitrary weight to distinguish QE proton in main program:
       WS = 0.01
       GO TO 1000
```

```
  300 CONTINUE
  c   Elastic event:
  c   Calculate Elastic angle (mrad) for proton:
        CALL RANNOR(O1,O2)                    ! Gaussian random numbers O1,O2
        RP = RP+ (197./(ATWT**0.3333))*O1/PC   ! Elastic angle in R plane[mr]
        ZP = ZP+ (197./(ATWT**0.3333))*O2/PC   ! Elastic angle in Z plane[mr]
  c   Assign an arbitrary weight to distinguish Elastic proton in main program:
        WS = 0.1

 1000 CONTINUE
        RETURN
        END
C.*************************************************************************
```

REFERENCES

1. A. Fasso, A. Ferrari, J. Ranft, and P.R. Sala, "FLUKA: a multi-particle transport code", CERN-2005-10 (2005), INFN/TC_05/11, SLAC-R-773.
2. N. Mokhov, "The MARS code system user's guide", Fermilab-FN-628, Fermi National Accelerator Laboratory (1995). MARS available on http://www-ap.fnal.gov/MARS/.
3. S. Agostinelli et al, "G 4 - a simulation toolkit", Nuc. Inst. Meth. A, Vol. 506, Issue 3, p. 250-303 (2003).
4. W. Scandale et al, Phys. Rev. ST - Accel. and Beams 11, 063501 (2008).
5. Review of Particle Physics, "Atomic and Nuclear Properties of Materials", p. 76-77 in the European Physical Journal C, Volume 3, Number 1-4, 1998.
6. J.D. Jackson, "Classical Electrodynamics", 2nd edition (Wiley, New York, 1975), pp. 647 ff.
7. E. Uggerhoj, "Channeling and Related Phenomena for GeV Particles", p. 5-37, in Relativistic Channeling, NATO ASI Series B, Physics Volume 165, edited by R.A Carrigan and J.A. Ellison, Plenum Press, New York, 1987.
8. K. Goulianos, "Diffractive Interactions of Hadrons at High Energies", Physics Reports, Vol. 101, No. 3, pp. 169-219, (1983).
9. R.J. Glauber and G. Matthiae, "High Energy Scattering of Protons by Nuclei", Nuclear Physics B21, pp. 135-157 (1970).
10. A. Van Ginneken, "Elastic scattering in thick targets and edge scattering", Phys. Rev. D37, 3292 (1988).
11. A. Schiz, et al, "Hadron-nucleus elastic scattering at 70, 125, and 175 GeV/c", Phys. Rev. D21, 3010 (1980).
12. M. Abramowitz and I.A. Stegun, Handbook of Mathematical Functions, p. 949, National Bureau of Standards, Applied Mathematics Series 55, Tenth Printing, December 1972.
13. J. Dawson, "Particle Simulation of Plasmas", Rev. Mod. Phys. Vol. 55, No. 2, p. 408-447, April 1983.
14. Igor Yazynin, Institute for High Energy Physics, Protvino, Russia, private communication; e-mail: Igor.Yazynin@ihep.ru.

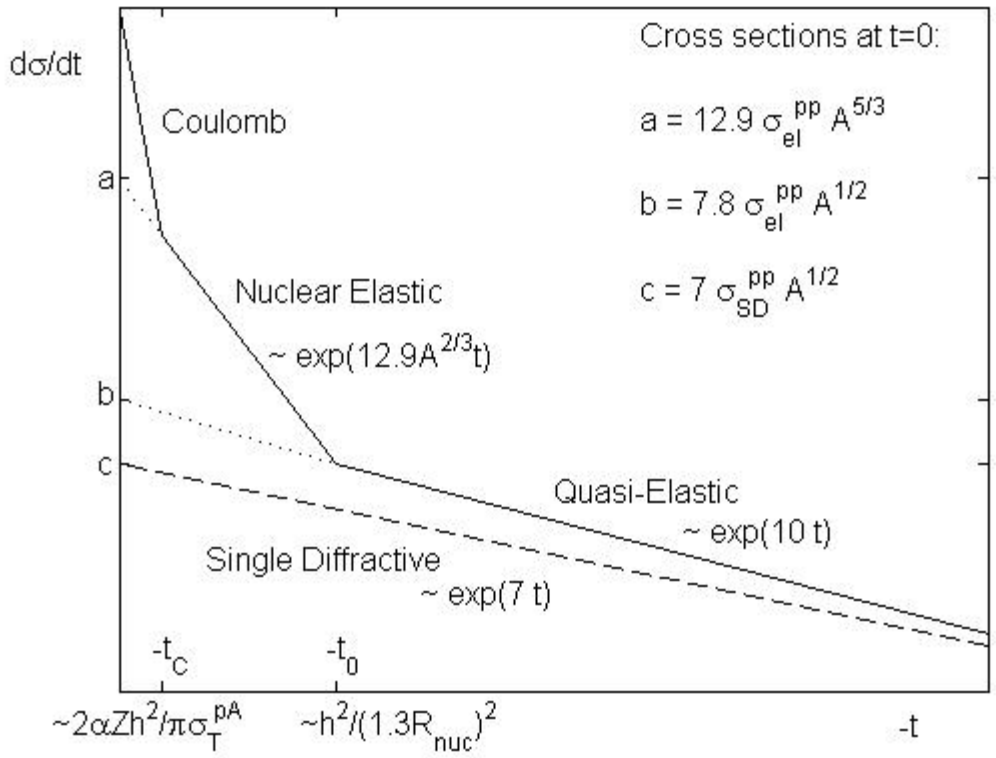

Figure 1. Simplified proton-nucleus differential cross sections for elastic, quasi-elastic, and single diffractive scattering versus $-t \approx p^2 \theta^2$ suitable for reduced-description, particle-matter simulations.

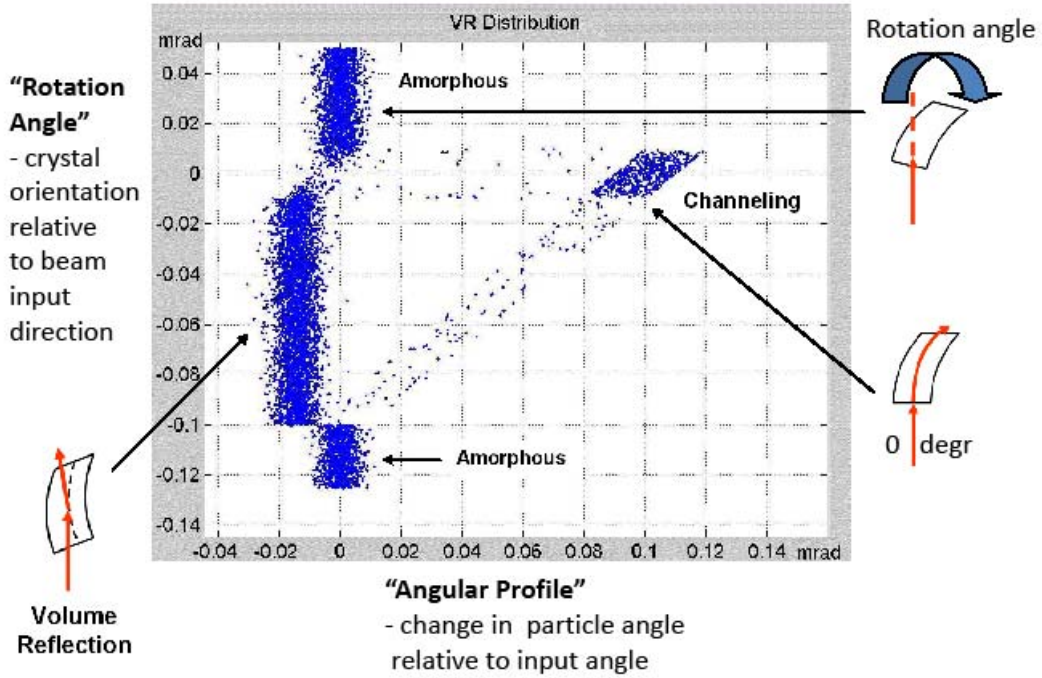

Figure 2. Simulated "triangle plot" in angle-space illustrating the different crystal channeling phenomena experienced by 400 GeV protons traversing a bent Si crystal (thickness 1mm, curvature radius 10 m). The vertical axis represents the angle between crystal plane orientation and the beam entry angle (0 degrees means crystal planes and beam aligned), and the horizontal axis measures the proton scattering angle relative to input angle (0 is no scattering). The diagonal band connecting the "Amorphous" and "Channeling" groups represent so-called volume-captured (VC) protons which have been scattered into a channel somewhere within the crystal volume. The horizontal band beginning at the "Channeling" group consists of dechanneled protons.

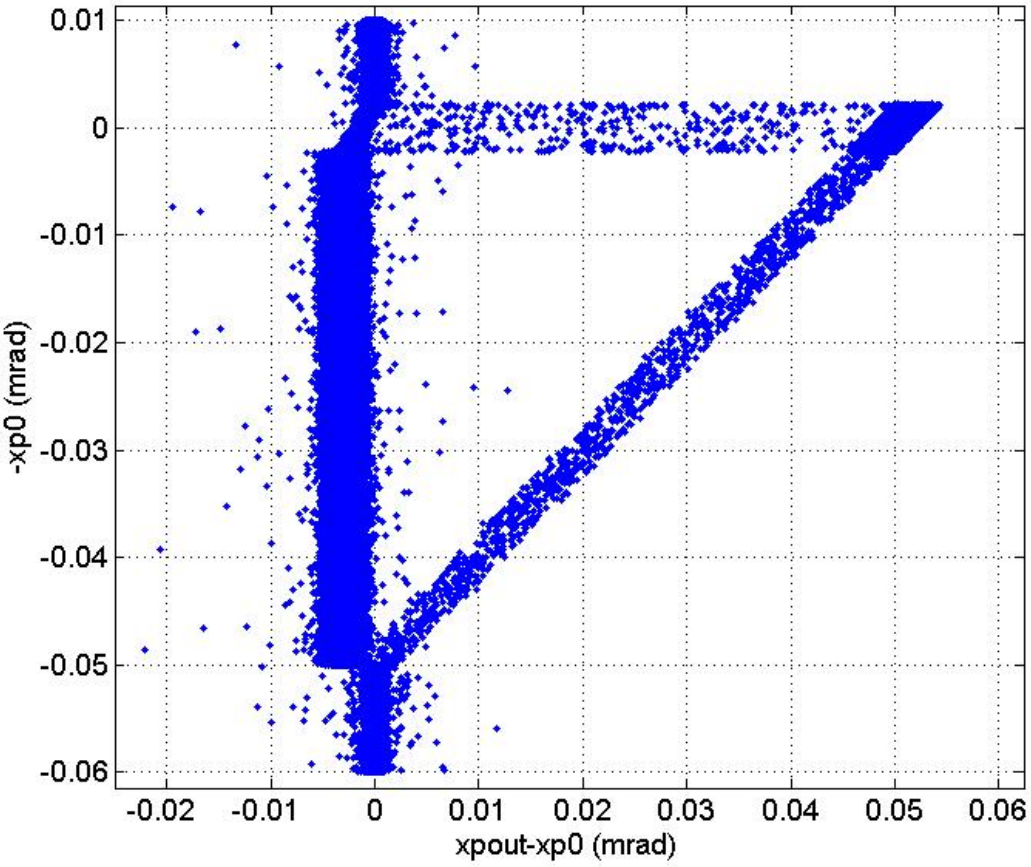

Figure 3. "Triangle plot" simulation in angle-space showing the different crystal channeling phenomena experienced by 7 TeV protons traversing a bent Si crystal, thickness 5 mm, and curvature radius 100 m. Nuclear effects are turned OFF and only MCS and large-angle Coulomb scattering are included for the 200K protons tracked here. The volume-reflected population is the vertical band shifted left at angles xp0 between 0 and 0.05 mrad. The average VR deflection is about 3 micro-rad.

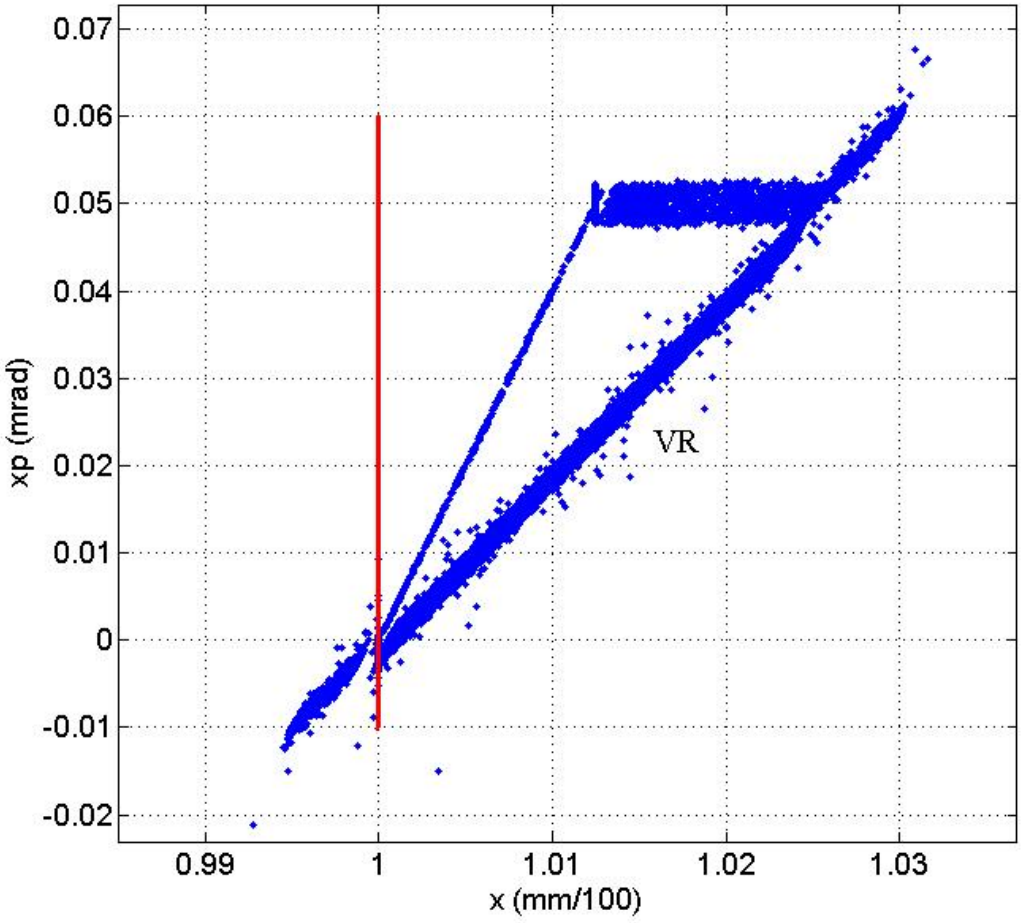

Figure 4. Transverse phase space at crystal exit for 7 TeV protons traversing a bent Si crystal, thickness 5 mm, and curvature radius 100 m. Nuclear effects are turned OFF and only MCS and large angle Coulomb scattering are included for the 200K protons tracked here. Vertical line at x = 0.01 mm represents the input phase space of the hypothetical halo beam slice, which has a range of angles xp from -0.01 mrad to 0.06 mrad. The volume-reflected population is the diagonal band marked VR at angles between 0 and 0.05 mrad.

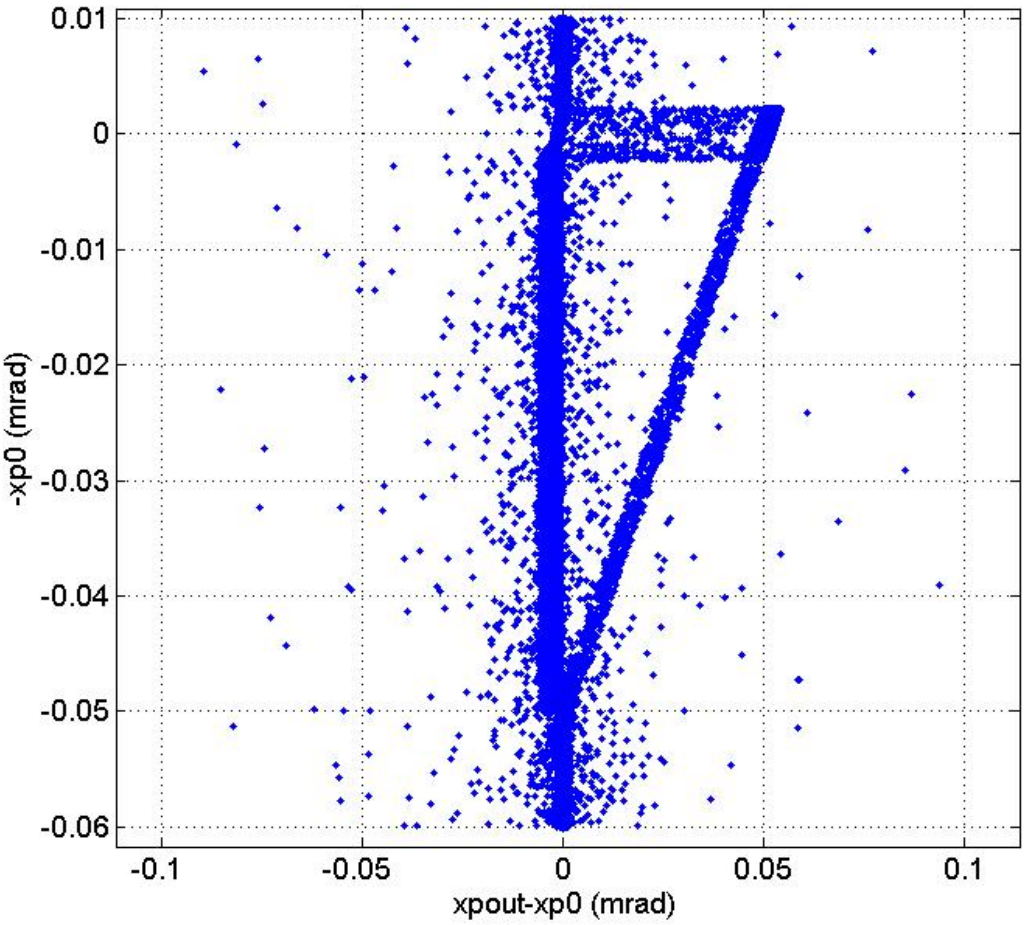

Figure 5. "Triangle plot" simulation in angle-space showing the different crystal channeling phenomena experienced by 7 TeV protons traversing a bent Si crystal, thickness 5 mm, and curvature radius 100 m. All nuclear and Coulomb effects are turned ON for the 200K protons tracked here. The volume-reflected population is the vertical band shifted left at angles xp0 between 0 and 0.05 mrad. The average VR deflection is about 3 micro-rad.

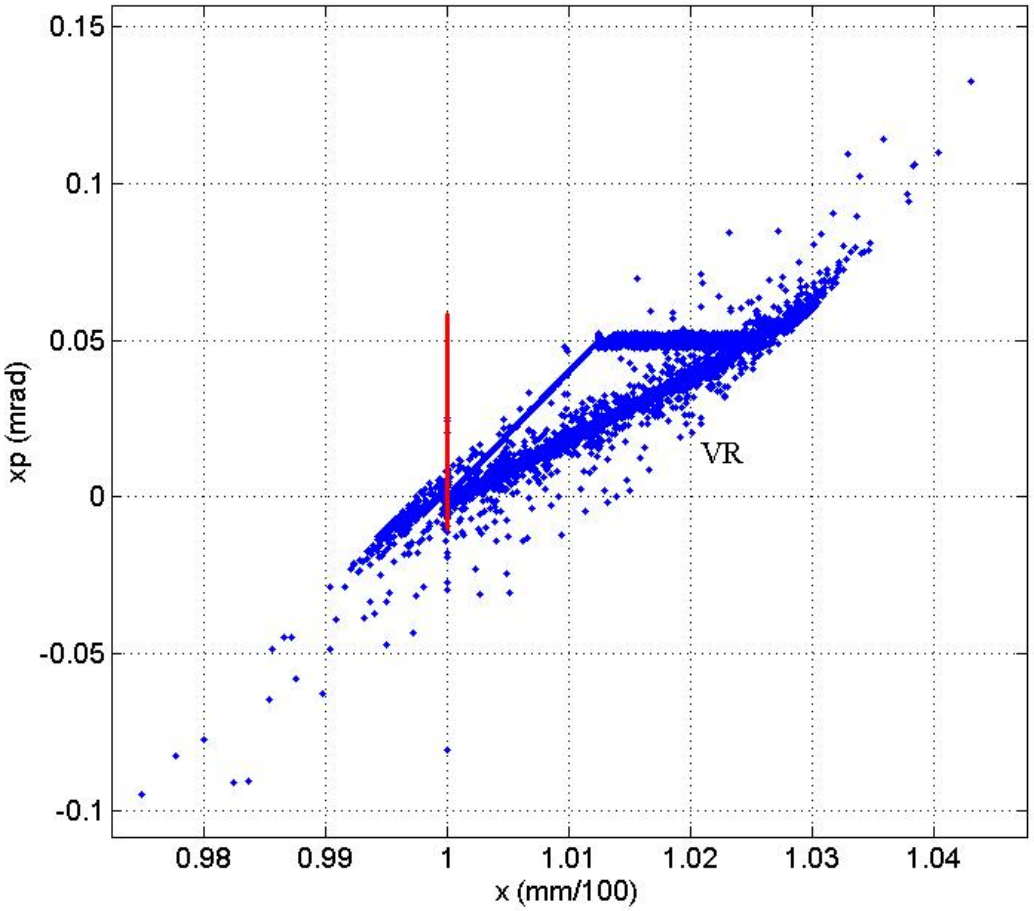

Figure 6. Transverse phase space at crystal exit for 7 TeV protons traversing a bent Si crystal, thickness 5 mm, and curvature radius 100 m. All nuclear and Coulomb effects are turned ON for the 200K protons tracked here. Vertical line at x = 0.01 mm represents the input phase space of the hypothetical halo beam slice, which has a range of angles xp between -0.01 mrad to 0.06 mrad. The volume-reflected population is the diagonal band marked VR at angles between 0 and 0.05 mrad.

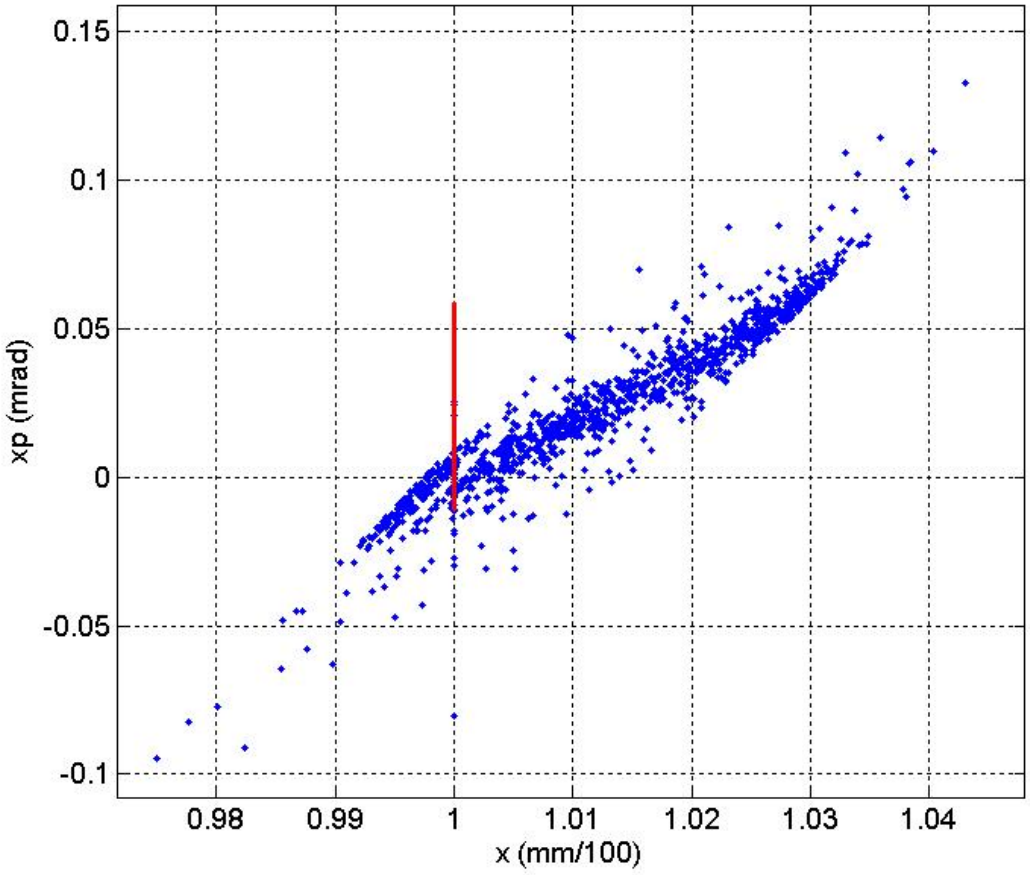

Figure 7. Transverse phase space at crystal exit showing nuclear scattered 7 TeV protons which survive passage through the bent Si crystal, thickness 5 mm, and curvature radius 100 m. Protons which did not undergo a nuclear scattering (fraction 0.985) and any absorbed protons (.0094) are omitted from this plot. The scattered beam fraction here is about 0.0056 of the 200K initial protons. Vertical line at x = 0.01 mm represents the input phase space of the hypothetical halo beam slice, which has a range of angles xp between -0.01 mrad to 0.06 mrad.